Microchim Acta (2008) 163: 49–56
DOI 10.1007/s00604-008-0950-0
Printed in The Netherlands

Microchimica Acta

Original Paper

Characterization of sub-systems of a molecular biowire-based biosensor device

Yang Liu[1], **Amit Gore**[1], **Shantanu Chakrabartty**[1], **Evangelyn C. Alocilja**[2]

[1] Department of Electrical and Computer Engineering, Michigan State University, East Lansing, MI, USA
[2] Department of Biosystems Engineering, Michigan State University, East Lansing, MI, USA

Received 17 October 2007; Accepted 24 December 2007; Published online 17 March 2008

Abstract. We describe the fabrication and characterization of components of a biosensor system that can be used for simultaneous screening of multiple pathogens in a sample. The two sub-systems are: (1) a mixed antibody immunosensor based on molecular biowires and (2) a multi-channel potentiostat for measuring conductance across the immunosensor. The immunosensor operates by converting binding events between antigen and antibody into a measurable electrical signal using polyaniline nanowires as labels and transducers. By mixing and patterning antibodies on a substrate, the response of the biosensor can detect the presence of either one of several pathogens present in the analyte through an equivalent change in conductance. The paper also presents a 42-channel potentiostat array which can be used for measuring the conductance change across the immunosensor. Each channel of the array uses a novel semi-synchronous $\Sigma\Delta$ modulator which enables detection down to femtoampere current ranges.

Keywords: Biosensor; polyaniline; nanowires; potentiostat

Correspondence: Yang Liu, Michigan State University, Department of Electrical and Computer Engineering, East Lansing, MI 48824, USA, e-mail: liuyang4@egr.msu.edu

Biosensors have emerged as important analytical tools for controlling disease outbreaks, which according to the United States Department of Agriculture (USDA) cause $2.9–$6.7 billion worth of losses every year [1]. A biosensor is a self-contained integrated device, which is capable of providing specific quantitative or semi-quantitative analytical information using a biological recognition element (biochemical receptor) which is retained in direct spatial contact with a transduction element [2]. Current research in biosensor technology has been focused towards investigating biosensors that demonstrate superior sensitivity, accuracy, reliability, high throughput and portability. In this regard, immunosensors (biosensors that use antibodies as biological recognition elements) are of great interest because of their applicability (any compound can be analyzed as long as specific antibodies are available) and high sensitivity. In particular, immunosensors with electrical readouts offer several advantages over their optical counterparts due to their reduced cost, reduced form factor and ease of signal acquisition. One such immunosensor which has been used in this paper was introduced in [3, 4] and has been shown to achieve a detection limit of 80 colony forming units (CFU) $\cdot$ mL^{-1} for bacteria and 10^3 cell culture infective dose per milliliter (CCID $\cdot$ mL^{-1}) of Bovine Viral Diarrhea Virus (BVDV) antigens in ap-

proximately 6 min. The immunosensor is disposable and relatively inexpensive to fabricate and operate, thus making it an attractive candidate for designing biosensors that can simultaneously detect multiple pathogens in food samples especially for the application of the point-of-care testing.

In literature, different architectures of multi-array biosensors have been proposed. One of the popular detection mechanisms relies on microarray technology and the use of optical readout for detecting hybridization events [5, 6]. Another multi-array detection which has been reported in [7] is based on a lateral flow immunosensor where multiple target-capture molecules are immobilized along the flow of the analyte. The technique, however, suffers from interference of preceding target capture zones and differences in signal intensity which decays along the direction of the flow. In [8], an electrokinetically-controlled heterogeneous immunoassay was developed for detecting multiple pathogens. Specificity experiments have been reported for three different pathogens where an optical device was used in the detection method. However, if the objective of the biosensor is to detect the presence of any one of several possible pathogens in a sample, a simplified architecture consisting of a mixture of antibodies could be used as a recognition layer. The mixture in conjunction with an electrical transducer can form an ''OR'' logical operation such that a signal is produced only in response to the presence of one or more target pathogens. The mixture of antibodies could then be patterned spatially across the biosensor to form a multi-array architecture.

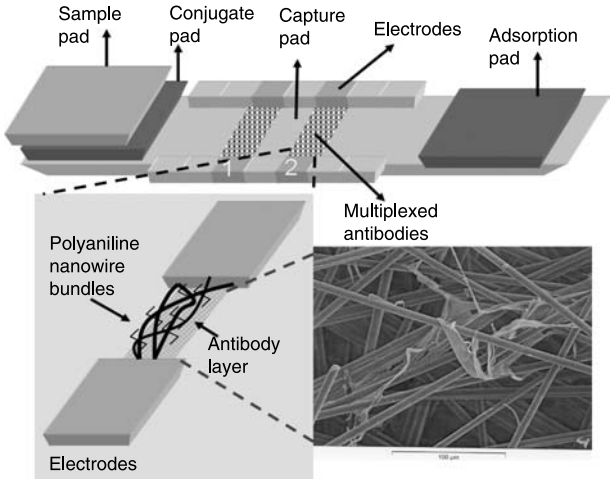

Fig. 1. The architecture of the proposed biosensor and a SEM image of the capture pad

Peripheral signal acquisition and measurement device is also important for conductimetric biosensors especially for applications in point-of-care testing. In this regard, multi-channel potentiostat integrated circuits (ICs) are ideal because the biosensor recognition element could be immobilized in proximity with the measurement circuitry, thus reducing artifacts produced by noise and interference. In literature, several multi-channel potentiostats have been proposed for electrochemical measurements. For instance in [9], a $\Sigma\Delta$ conversion approach has been used for measuring currents generated due to neuro-chemical reactions. An integrating analog-to-digital conversion technique has been used in [10] for cyclic voltammetry based measurements and has been demonstrated for sensi-

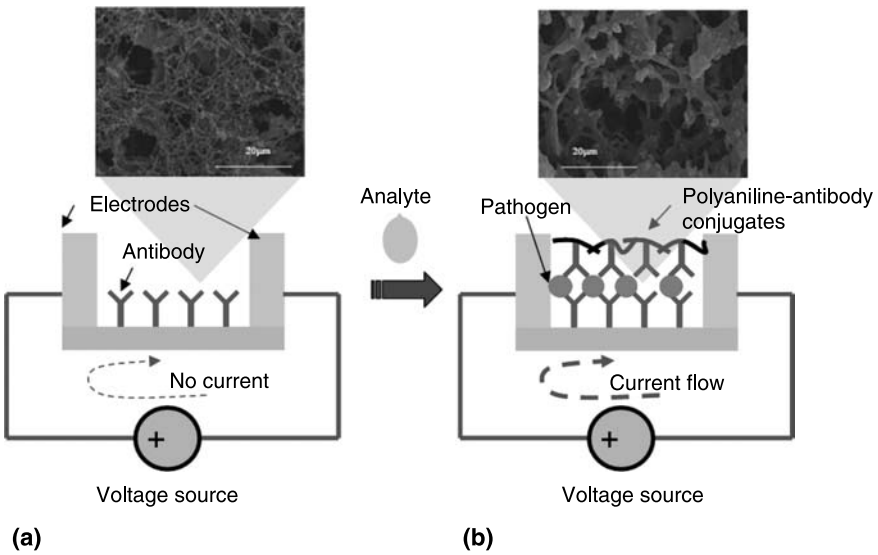

Fig. 2. Principle of operation of the biosensor with illustration of the two states by SEM images

tivity down to picoamperes of current. Integrated and implantable potentiostats have been reported for glucose concentration measurement with accuracy of nanoamperes [11]. For the multi-array biosensor proposed in this paper, we reuse the design of our previously reported potentiostat that employs a semi-synchronous $\Sigma\Delta$ modulator [12]. The architecture combines asynchronous time-encoding machine (TEM) [13] with a continuous time $\Sigma\Delta$ (CT$\Sigma\Delta$) conversion [14] to facilitate the measurement of currents down to few femtoamperes.

Experimental

Principle of the biosensor

The architecture of a molecular bio-wires based biosensor is shown in Fig. 1. It consists of four pads: sample application pad, conjugate pad, capture pad, and absorption pad. The capture pad or the area that immobilizes the recognition elements consists of several antibody capture zones. The SEM image of the conjugation of antibody-polyaniline is also shown in the sub-image of Fig. 1, where polyaniline nanowires appear to be rod-shaped. The principle of operation of a single pathogen (single antibody) and single strip biosensor is illustrated in Fig. 2a, b, which shows a cross-sectional view of the antibody strip. There is an open channel between two electrodes across the capture pad before any analyte is applied on the sample pad. Immediately after sample is applied to the sample pad, the solution containing the antigen flows to the conjugate pad, dissolves with the polyaniline-labeled antibody (Ab-P) and forms an antigen-antibody-polyaniline complex. The complex is then transported by a capillary action into the capture pad containing the immobilized antibodies. If the antigens bind with their specific antibodies on the capture pad, the second antigen-antibody reaction forms a sandwich as shown in Fig. 2b. The polyaniline nanowires extend out to bridge adjacent cells and lead to conductance change between the electrodes (Figs. 1 and 2b). The conductance change is determined by the number of antigen-antibody bindings, which is related to the antigen concentration in the sample. The unbounded non-target organisms are subsequently separated by the capillary flow to the absorption membrane. The conductance change is sensed as an electrical signal (current) across the electrodes. Figure 2a, b also show SEMs of the capture pad before and after the analyte with pathogen has been applied. The change in material texture can be observed in Fig. 2b which is attributed to the formation of the antibody-antigen-antibody-polyaniline complex connecting the electrodes.

Construction materials

Purified rabbit polyclonal antibodies against *B. cereus* and *E. coli* were obtained from Meridian Life Science (Saco, ME, USA). The antibodies were suspended in phosphate buffer solution (pH 7.1) and stored at 4 °C. *B. cereus* and *E. coli* strains were obtained from the National Food Safety and Toxicology Center (Michigan State University) and the Michigan Department of Community Health (East Lansing, MI, USA). A 10 μL loop of each isolate was cultured in 10 mL of nutrient broth and incubated for 24 h at 37 °C to prepare stock cultures. The stock cultures were serially diluted with 0.1% peptone water to obtain varying concentrations of each microorganism. Polyaniline was purchased from Sigma-Aldrich (St. Louis, MO, USA). All experiments were carried out in a certified biological safety label II laboratory. The sample pads (size: 20 mm × 5 mm), capture pads (size: 20 mm × 5 mm), and absorption pads (size: 15 mm × 5 mm) were made of nitrocellulose membrane and the conjugate pads (size: 10 mm × 5 mm) were made of fiberglass membrane (grade G6). The porous nitrocellulose substrate ensures good adsorption properties for immobilized antibodies and allows non-target antigens to flow through. The conjugate pad was designed to allow maximal adsorption and flow of polyaniline-conjugated antibodies. Antibody concentration used for conjugate pad was $150\,\mu g \cdot mL^{-1}$ and for the capture pad was $500\,\mu g \cdot mL^{-1}$. All these values were found to be optimal, resulting in the highest ratio between the number of captured cells and the actual cell concentration tested.

Labeling of antibodies

The polyaniline-antibody conjugates were prepared by suspending 800 μL of the mixture of the polyclonal antibody against *B. cereus* and *E. coli* (concentration $150\,\mu g \cdot mL^{-1}$) in a 4 mL of polyaniline solution ($50\,mg \cdot mL^{-1}$) in phosphate buffer (pH 7.1) containing 10% dimethylformamide (DMF) (v/v) and 0.1% LiCl (w/v). The solution was incubated at room temperature for 1 h to allow binding of the antibodies with polyaniline and then treated with a blocking reagent (Tris buffer containing 0.1% casein). The polyaniline-antibody conjugates were then precipitated by centrifugation at 12,000 rpm for 5 min. The supernatant fluid was discarded and the pellets were mixed with the blocking reagent and centrifuged again. The centrifugation step was repeated three times. The conjugates were finally suspended in phosphate buffer solution containing 0.1% LiCl (w/v) and 10% DMF (v/v) and stored at 4 °C until used. The conjugate pads were prepared by soaking the fiberglass strip into the conjugation solution till homogenous dispersion is achieved.

Immobilization of antibodies

Before dispensing the antibody mixture, the capture pads were pretreated with distilled water and 10% (v/v) methanol sequentially and left to dry for 1 h. Then, the pad was treated with 0.5% (v/v) glutaraldehyde and left to dry again. Subsequently, the mixture of the polyclonal antibody against *E. coli* and *B. cereus* were immobilized on the capture pads using dispensing machine (Kinematics Automation Inc.) and incubated at 37 °C for 1 h. 0.1 mM tris buffer (pH 7.6, containing 0.1% (v/v) Tween–20) were dispensed onto the capture pad to remove and block residual functional groups. The pads were then incubated at 37 °C for 45 min.

Fabrication of electrodes

We have tried several methods to make electrodes onto the nitrocellulose membrane (capture pad) including screen printing and using silver conductive pastes. Recently, we adopt the method of aluminum evaporation technique, which use non-destructive manner to evaporate aluminum particles onto the nitrocellulose membrane. Figure 3 shows the sample of the mask, the aluminum electrodes dispensed onto the membrane and the fabricated biosensor with the single pair of electrodes. Mask is put onto the nitrocellulose membrane to separate aluminum electrodes. Once aluminum electrodes are pattern onto the membrane, immobilization of antibody is treated followed the procedures in the last subsection.

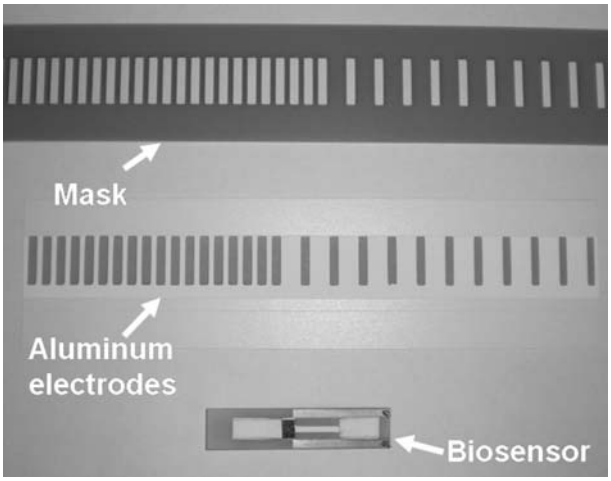

Fig. 3. Copper masks which have been used for making electrodes

Conductance measurement

We have previously reported a semi-synchronous ΣΔ modulation algorithm [12] that could be for acquiring and measuring currents down to femtoampere levels. For the proposed biosensor, the semi-synchronous ΣΔ modulator as a potentiostat by measuring current directly at a reference electrode while maintaining it at a virtual ground. The architecture of the modulator configured as a potentiostat is shown in Fig. 4, which consists of an operational amplifier in a feedback configuration (using a capacitor C). The inverting terminal of the opamp (node A) is thus always maintained at a constant potential (V_{ref}). The other end of the biosensor electrode is maintained at a constant potential (V_{meas}) which ensures that the current flowing into the potentiostat is proportional to the conductance of the biosensor according to:

$$I_{in} = G_{bio}(V_{meas} - V_{ref}). \quad (1)$$

With G_{bio} being the transconductance of the biosensor.

We now briefly describe the semi-synchronous ΣΔ algorithm for which the readers are referred to Ref. [12] for details. The semi-synchronous algorithm consists of a synchronous conversion step, followed by an asynchronous compensation step. During the synchronous conversion step, a combination of input current and a reference current (I_{ref}) is first integrated on a capacitor (shown in Fig. 4a) for every clock cycle. Without loss of generality we will assume $V_{ref} = 0$. If the output of the opamp is denoted by U_n where $n = 1, 2, \ldots, N$ represents indices of clock cycles, then at each clock cycle the following relationship holds

$$U_n = U_{n-1} + \left(\frac{I_{in}}{I_{ref}} - D_n\right)\frac{I_{ref}T_{clk}}{C} \quad (2)$$

with T_{clk} being duration of each clock period and $D_n \in \{-1, +1\}$ is a Boolean variable that controls the switches S_1 and S_2. The value of D_n is updated by thresholding U_n using a hysteretic comparator according to

$$D_n = \text{sign}(U_{n-1} + D_{n-1}\Delta) \quad (3)$$

where Δ denotes the hysteresis level of the comparator. The uniqueness of using a hysteretic comparator as opposed to standard comparators used in conventional ΣΔ modulation is that the value of D_n not only depends on U_n but also on the previous values of the comparator output (illustrated in Fig. 4b). This ensures that the integrator voltage satisfies $|Un| > \Delta$ before the output of the comparator switches. For sufficiently low magnitude of $I_{ref}T_{clk}/C \gg \Delta$, the integrator output exhibits significantly higher switching cycles as compared to a converter operating with a larger magnitude of Δ. The reduction in switching cycles also reduces substrate noise and integrator non-linearity, which are important for measurement of ultra-low magnitude input currents. The counter in Fig. 4a counts the number of digital pulses D_n which is a digitized representation of the input current.

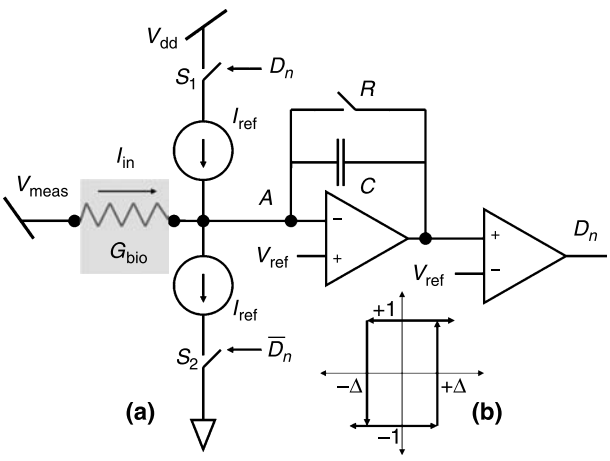

Fig. 4. Architecture of a semi-synchronous ΣΔ modulator which interfaces with the immunosensor (represented by a conductance)

Results and discussions

Characterization of the potentiostat array

A prototype consisting of an array of 42 potentiostats has been fabricated in a 0.5 μm CMOS process. The

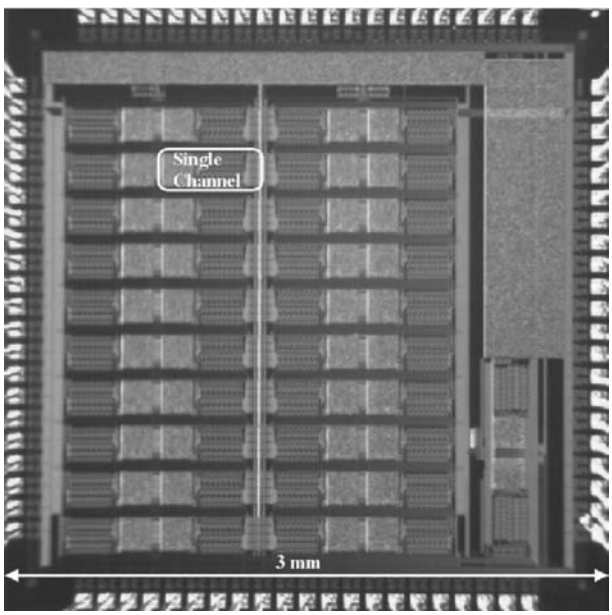

Fig. 5. Micrograph of the multi-channel potentiostat interface

size of the prototype is 3 mm × 3 mm and its micrograph is shown in Fig. 5. The active area occupied by a single semi-synchronous ΣΔ converter is 0.085 mm^2 which makes it one of the most area efficient potentiostats reported in the literature. Table.1 summarizes the specification of the multi-channel potentiostat chip. The first set of experiments was used to measure the resolution of the semi-synchronous ΣΔ converter. A GPIB controlled current source from (*Keithley Instruments*) was used to generate currents. For this experiment, the hysteresis level of the comparator was fixed to Δ = 100 mV. Figure 6 shows the differential non-linearity (linear regression error) measured using with the prototype potentiostat, where each least significant bit (LSB) corresponds to 80 pA. This demonstrates that the potentiostat can achieve a resolution of 10 bits for a dynamic range of 100 nA. Sensitivity measurements (minimum detectable current) were performed using an on-chip pMOS transistor with adjustable gate-to-source voltage, which has been shown to be capable of generating femtoampere range currents [15]. The use of internal current source avoids unnecessary coupling from external noise sources, which is critical for ultra-small current measurements. Figure 7 shows a log linear plot of the digitized output produced by the semi-synchronous ΣΔ converter when the gate-to-source of the pMOS transistor is varied. Landmark gate voltages were mapped onto current values using an external pico-ammeter and are indicated on the graph. Figure 7 shows that the potentiostat can measure sub-threshold currents up to 50 fA range.

Table 1. Measured specification using the prototype of multi-channel potentiostat

Parameters	Values
Technology	0.5 μm 2P3M CMOS
Size	3 mm × 3 mm (42 Channels)
Supply	3.3 V
Channels	42
Input current range	−100 to 100 nA
Resolution	10 bits
Sensitivity	50 fA
Active area	0.085 mm^2 (1 Channel)

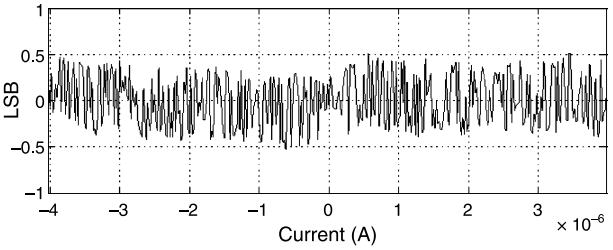

Fig. 6. Measured DNL plot for a semi-synchronous ΣΔ converter

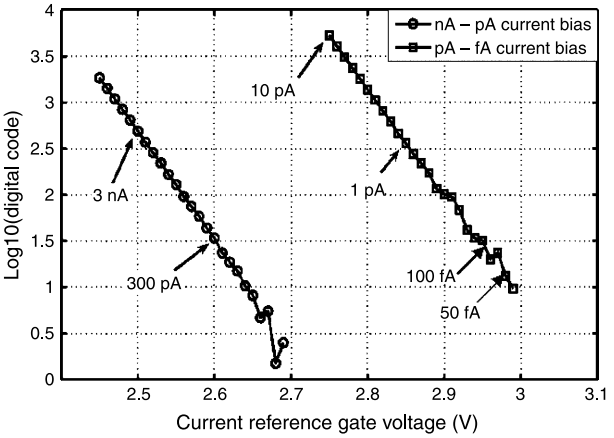

Fig. 7. Demonstration of the potentiostat for measurement of sub-threshold characteristics of a p-MOS transistor, whose drain current can be as low as fA

We have interfaced the fabricated prototype with our previously reported biosensor and have used it for measurement of conductance variations transduced by antigen-antibody bindings [12].

Characterization of the biosensor

As a proof of concept we have patterned the mixtures at only two spatial locations on the capture pad, which we will designate by 1 and 2 (as shown is Fig. 1) as indicated in the measurement results. Strip 1 is antibody capture zone, which is close to the conjugation pad while strip 2 is a little bit far from the conjugation pad. Even though the experiments in this paper have

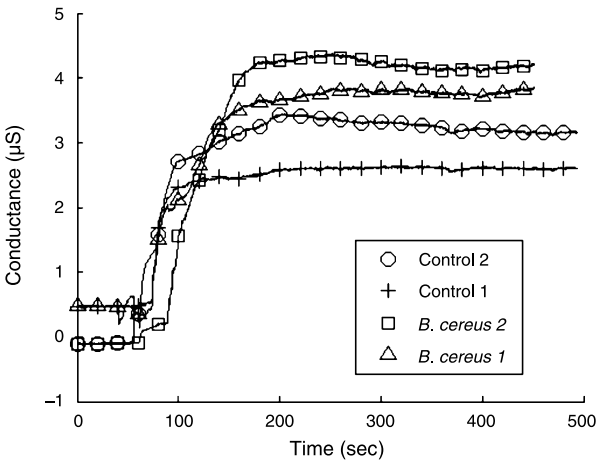

Fig. 8. Conductance measured across two antibody capture zones (marked by 1, 2) when an analyte containing *B. cereus* is applied

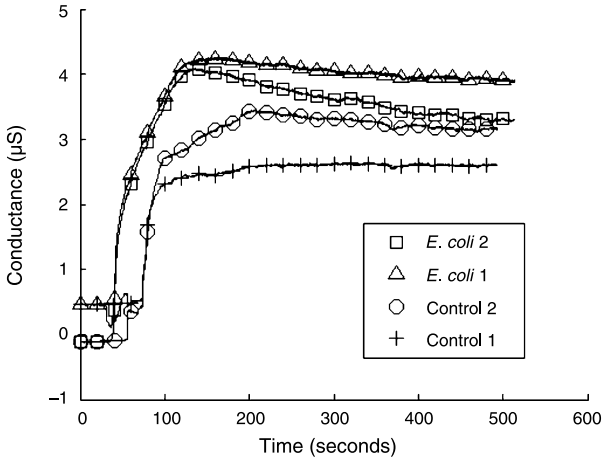

Fig. 9. Conductance measured across two antibody capture zones (marked by 1, 2) when an analyte containing *E. coli* is applied

used only two pathogens (*B. cereus* and *E. coli*), the proposed principle can be extended to include antibodies specific to other pathogens.

Figures 8–10 show typical responses where the conductance across the two antibody capture zones are simultaneously measured (marked by 1, 2 in Fig. 1) as a function of time. For comparison, conductance corresponding to a control solution (analyte without pathogens) is also plotted on the figures. In Figs. 8–10, Control 1, *E. coli* 1, *B. cereus* 1, and Both 1 represent the conductance measured across antibody capture zone 1 (marked in Fig. 1) when control solution, *E. coli*, *B. cereus*, and the mixture of *E. coli* and *B. cereus* solution are applied. Similar notations (Control 2, *E. coli* 2, *B. cereus* 2, and Both 2) also hold for strip 2 in the Figs. 8–10. For these experiments, the concentrations of *B. cereus* and *E. coli* were calibrated to be 6×10^7 CFU $\cdot$ mL^{-1} and 5×10^7 CFU $\cdot$ mL^{-1} respectively. Confirmation of the pathogens followed standard microbiology protocols [16]. For this purpose, colonies were counted using an automated platter-counter in a biosafety level II environment. All laboratory and biohazard waste were labeled, handled, and disposed of according to the MSU standard procedures for handling biohazardous waste [17]. It can be seen from Figs. 8–10 that the conductance measured across both of the antibody capture zones are higher when either of the pathogen is present compared to the control. This verifies the functionality of the multi-OR biosensor. Because the antibody zones are located at different spatial locations, the conductance measured across zone 1 and zone 2 changes sequentially between 40 and 90 sec. Figures 8–10 also show interference of measured conductance due to electrical interaction between the two electrodes. However, this interference does not significantly impact the ability of the biosensor to discriminate between pathogenic and non-pathogenic samples. Figure 11 shows the conductance measurement across a single antibody capture zone when samples containing different concentrations of pathogens are applied. Every test is repeated three times and the error bars show the standard deviation. The measured results thus verify the functionality of the mixed antibody strip to detect either one of the two pathogens at different concentration levels.

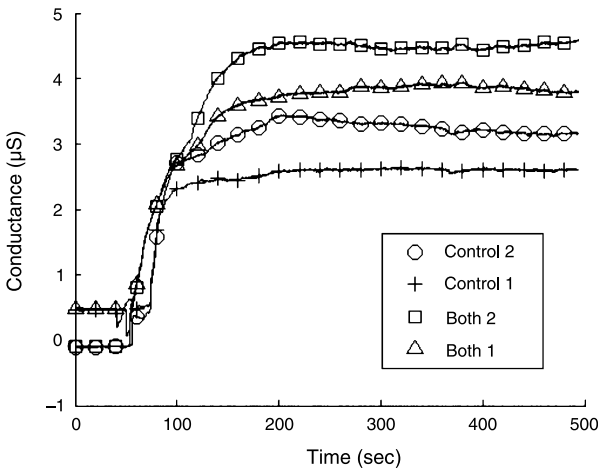

Fig. 10. Change in conductance across two antibody capture zones (marked by 1, 2) when both pathogens (*B*: *B. cereus*, *E*: *E. coli*) are present

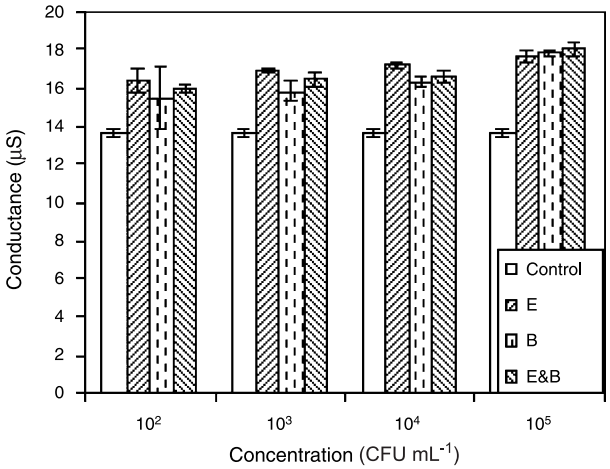

Fig. 11. Change in conductance across the mixed antibody biosensor for different concentration of pathogens (*B: B. cereus*, *E*: *E. coli*)

Miniaturization and sensitivity of the potentiostat

Using the measured conductance, we derived a first-order electrical model for the conductance measured across the single antibody capture zone of the biosensor (Fig. 1) as a function of the pathogen concentration in the sample. This is expressed as:

$$G_{\text{bio}}(X) = G_0 + \kappa_B \log \frac{X_B}{X_{0B}} + \kappa_E \log \frac{X_E}{X_{0E}} \qquad (4)$$

where X_B and X_E represents the concentration of the *B. cereus* and *E. coli* in CFU $\cdot$ mL^{-1}, G_0 represents the ''control'' transconductance, κ_B, κ_E represents sensitivity factors and X_{0B}, X_{OE} are detection constants corresponding to pathogens *B. cereus* and *E. coli*. Note that Eq. (4) is valid only for $X_B \geq X_{0B}$, $X_E \geq X_{0E}$, which is a reasonable assumption. Based on the Eq. (4), the change in conductance can be expressed as a function of change in concentration δX_B, δX_E with respect to a reference concentration X_{rB}, X_{rE} as

$$\begin{aligned} \delta G &= \kappa_B \log\left(1 + \frac{\delta X_B}{X_{rB}}\right) + \kappa_E \log\left(1 + \frac{\delta X_E}{X_{rE}}\right) \\ &\approx \kappa_B \left(\frac{\delta X_B}{X_{rB}}\right) + \kappa_E \left(\frac{\delta X_E}{X_{rE}}\right) \end{aligned} \qquad (5)$$

The incremental relationship given by Eq. (5) shows a linear variation of the incremental conductance with respect to an incremental concentration change. Using typical values of constants presented in Ref. [18], it can be calculated that a 0.1% variation in concentration would require measuring a change of 1 nA of current. The requirement becomes even more stringent (≤ 10 pA) when the width of the antibody strip is reduced to accommodate a large array of antibody strips. This motivates the design of ultra-sensitive potentiostats that can measure small changes in current produced by change in biosensor conductance.

Conclusions

In this paper we characterized sub-systems of a biosensor device that can be used for rapid screening of multiple pathogens in an analyte. The core principle behind the proposed architecture is the computational primitive inherent in antigen-antibody interaction which leads to a transistor like operation. By mixing two different antibodies together and patterning them along different spatial locations, a logic ''OR'' function was implemented which was demonstrated to detect the presence of one or more target pathogens. One of the limitations in using mixture of antibodies in screening of multiple pathogens is the reduced sensitivity due to limited availability of binding sites for target pathogens. However, this artifact can be compensated by enhancing the sensitivity of the potentiostats which was one of the salient topics in this paper. Also, analyte reaching the antibody strips located at spatially disjoint locations contain variable concentration of pathogens which produce a weaker measurable signal. This observation has been reported in [8], and a solution proposed to remedy this problem was a symmetric architecture which ensures a uniform flow of pathogens towards the recognition sites. Even in this case, the pathogen concentration per strip reduces which again motivates the design of ultra-sensitive potentiostats. In this paper, we have used a potentiostat array which uses a semi-synchronous $\Sigma\Delta$ conversion algorithm for measuring change in conductance. Using a fabricated prototype, each of the potentiostat channels has been shown to achieve femtoampere range sensitivity in current measurement making it ideal for future work towards miniaturizing the proposed biosensor device.

Acknowledgements. This work is supported in part by a research grant from the National Science Foundation: NSF ECCS-0622056.

References

1. Food and Drug Administration (2000) Bacteriological analytical manual, 8th edn. Association of Analytical Chemists, Arlington, VA
2. IUPAC (1999) Electrochemical biosensors: recommended definitions and classification. Pure Appl Chem 71: 2333
3. Muhammad-Tahir Z, Alocilja E C (2003) A conductometric biosensor for biosecurity. Biosen Bioelectron 18: 813
4. Muhammad-Tahir Z, Alocilja E C (2003) Fabrication of a disposable biosensor for *Escherichia coli* o157:H7 detection. IEEE sensor J 3: 345
5. Wiese R, Belosludtsev Y, Powdrill T, Thompson P, Hogan M (2001) Simultaneous multianalyte ELISA performed on a microarray platform. Clini Chem 47: 1451
6. Taitt C R, Golden J P, Shubin Y S, Shriver-Lake L C, Sapsford K E, Rasooly A, Ligler F S (2004) A portable array biosensor for detecting multiple analytes in complex samples. Microbial Ecol 47: 175
7. Malamud D, Bau H, Niedbala S, Corstjens P (2005) Point detection of pathogens in oral samples. Adv Dent Res 18: 12
8. Gao Y, Hu G, Lin F Y H, Sherman P M, Li D (2005) An electrokinetically-controlled immunoassay for simultaneous detection of multiple microbial antigens. Biomed Microdevices 7: 301
9. Murari K, Stanacevic M, Cauwenberghs G, Thakor N V (2005) Integrated potentiostat for neurotransmitter sensing. IEEE Eng Med Biol Mag 24: 23

10. Narula H S, Harris J G (2004) VLSI potentiostat for amperometric measurements for electrolytic reaction. ISCAS 1: 457
11. Beach R D, Conlan R W, Godwin M C, Moussy F (2005) Towards a miniature implantable in vivo telemetry monitoring system dynamically configurable as a potentiostat or galvanostat for two- and three-electrode biosensors. IEEE T Instrum Meas 54: 61
12. Gore A, Chakrabartty S, Pal S, Alocilja E C (2006) A multichannel femtoampere-sensitivity potentiostat array for biosensing applications. IEEE T Circ Syst 53: 2357
13. Kinget P R, Lazar A A, Toth L T (2005) On the robustness of an analog VLSI implementation of a time encoding machine. ISCAS 5: 4221
14. Razavi B (1995) Principles of data conversion system design. Wiley, New York, p 220
15. Linares-Barranco B, Serrano-Gotarredona T (2003) On the design and characterization of femtoampere current-mode circuits. IEEE J Solid St Circ 38: 1353
16. FDA-Food and Drug Administration (2000) Bacteriological analytical manual. AOAC International, Gaithersburg, MD
17. Michigan State University (1998) Biosafety manual. Office of Radiation, Chemical, and Biological Safety
18. Liu Y, Chakrabartty S, Alocilja E C (2007) Fundamental building blocks for molecular bio-wire based forward-error correcting biosensors. Nanotech 18: 424017